RESEARCH ARTICLE

DOI: 10.34256/ijcci2223

International Journal of Computer Communication and Informatics

An Inventive Method to Fabric Part Structural Defect Detection Using Frame Harmonizing

M. Dhivya [a, *], D. Suganthi [a]

[a] Department of Computer Science, PSGR Krishnammal College for Women, Coimbatore, Tamilnadu.

* Corresponding Author: dhivyam@psgrkcw.ac.in

Received: 08-09-2022, Revised: 26-09-2022, Accepted: 18-10-2022, Published: 30-12-2022

Abstract: Using a frame harmonizing based approach, this paper examines paper defects. In the textiles industry, the quick cutting and sewing of fabric has resulted in a lot of small mistakes, making this task extremely difficult. Especially these deformities won't be quickly recognized by specialists as well as programming. A novel frame harmonizing method is used in our system to find flaws in the fabric production process. Transformation and filtering techniques are used for the inputted fabric image frame. The conventional outline extraction method Berkeley edge detector is used to extract the edge map. Contour-based features are extracted and classified by K-Nearest Neighbour (KNN) classifier. The experimentation with real-time data set produced the outstanding performance results when compared with state of the art methods.

Keywords: Fabric fault, Defect detection, Classification, Edge detection.

1. Introduction

Manufacturing relies heavily on the detection of industrial defects. Fabric defect control is the primary component of textile industry quality control, and fabric defect detection is a crucial step in the quality control section. The processing costs of the fabric would be significantly impacted by this. The auditors' mental and physical state can easily influence fabric inspection by human sight. Quality assurance is essential for promoting the product's competitive advantage in the face of fierce competition in the textile industry. One of the most developed areas in the textile quality control industry is automated fabric defect detection. To address this problem, a variety of methods for detecting flaws in the fabrics were suggested. A fundamental issue is the development of a flexible, knowledgeable, dependable, integrated, and continuous vision framework for textile manufacturers' quality control procedures. For fabric defect detection, numerous model-based approaches have been presented.

Piezo ceramic Sensors (PZT) were used to monitor transmitted waves using the linear wave scans mechanism [1]. A structural texture analysis approach, the blob detection technique [2] takes into account aspects of the Human Visual System (HVS) when detecting a wide range of textile flaws. A threshold of acceptable differences in the properties of blobs based on human perception is used to identify flaws. The automatic fabric evaluation system evaluates woven fabric structure and quality automatically [3]. The Local Contrast Deviation (LCD) approach for fabric defect detection [4] was proposed to describe features of the contrast difference in four directions between the analysed image and a defect-free image of the same fabric with a bi-level threshold function for defect segmentation.

Texture features based on the Gabor wavelet network [5] are used to get rid of the background fabric and find the defects. Using the aforementioned characteristics, the pre-trained system constructs the structuring elements. The most important values for identifying flaws in the textured image are the texture features. After co-occurrence features are extracted from the decomposed fabric textured image, a Mahalanobis distance classifier is trained with the features of annotated samples from the work [6].For the estimation of fundamental normal frequencies, a method for evaluating the integrity of structures in a non-destructive manner [7] is utilized. By communicating the exchange that takes place between execution and computational load, another brand-new data fusion strategy was proposed [8] to multiplex the data that comes from various channels. Because of the improved binary, textural, and neural network algorithms [9], it was possible to find a wide variety of fabric flaws in real-world modern conditions, where the proximity of a wide variety of noises is a foregone conclusion. A simulated fabric model [10] was used to comprehend the connection between the texture structure in picture space and the recurrence space, where Fourier transforms are connected to monitor the fabric's spatial frequency spectrum.

The author [11, 12] presents a multi determination approach for the assessment of local abandons is inserted in uniformly textured surfaces based on an efficient wavelet transforms-based image restoration strategy. A Gabor wavelet network (GWN) is used to optimally extract texture features from a non-imperfect fabric image when planning the Gabor filters for a new defect detection method [13]. The programmed investigation of imperfections in haphazardly textured surfaces [11] relies on Using a collection of fabric images taken from a database containing a wide variety of fabric images, the implementation of their deformity detection scheme was evaluated offline. A PC-based real-time inspection framework with high detection rates and minimal effort was proposed [14]. In [15,16], a framework and fault detection algorithm for automated textile visual inspection were proposed. Modern vision frameworks need to work slowly, have a low rate of false positives, and be able to adapt to different types of exam locations. This served as the foundation for the creation of a fabric structural defect detection algorithm that makes use of the frame harmonizing strategy.

Generally speaking, what a PC vision evaluation system researches and controls is that of specific items. As a result, we are able to select suitable technology and reorganize the execution procedure based on prior knowledge of the performed fundamentals, which is also sufficiently understood to fulfill the task's goal. We employ the outline orchestrating construct approach based on texture imperfection review as follows, in accordance with the previous information separated from the shape of the fabric frame.

There are four sections to the methodology: The methods of image pre-processing that are used for enhancement are discussed in section I. The part II portrays the location strategy Berkeley edge indicator for edge map. The process of extracting contour features is explained in section III. The classification method used to achieve the best results is discussed in section IV.

2. Methodology

As a result, we have developed a Frame Harmonizing approach-based system in this study for automatic structural defect detection in fabric parts. For this purpose, real-time fabric images are gathered from the fabric production industries.The affine transformation is used to correct distortions during image capture. Pre-processing techniques employ a guided filter to enhance the edges. In the pre-processed images, the Berkeley edge detector is used to locate the boundaries of fabric. Regardless of the color attribute, an image's edge map carries the image's solid structure. After extracting contour features from the edge map using statistical and transformation-based techniques, a KNN classifier is trained to classify the defect category.

3. Data Set Description

The fabric production industries, such as "Hershees Men's Designer" and "Finela Designers," provide the real-time fabric images. As per the meeting with the people groups who are including in the texture creation and organization process, the texture deserts are primarily distinguished while on the texture yet it's excessively challenging to recognize when it emerges fundamentally. Therefore, 10 samples of each fabric's components are gathered after the parts are first listed. At a fixed distance of one meter and an angle of 90 degrees to the surface of the fabric part, a standard 7 MP digital camera is used to capture the images.An image has a resolution of 3072 x 2304. There are 15 distinct types of fabrics, each with 64 fabric parts and 640 images. The state of the fabric is used to label the entire dataset. The standard texture part likewise caught for every one of the 64 sections. Thus, there are 704 images in total in the fabric DB.

I. PRE-PROCESSING

Affine transformation

Pre-handling steps are performed prior to the edge location process to ensure that the information picture remains size- and revolution-independent. Even though the camera and texture input outline are fixed, a non-ideal arrangement of the texture on the casing may cause mathematical bends or disfigurements. Our work uses an affine transformation to avoid such distortions.

The fabric frame is transformed into a standard invariant input frame using the linear mapping technique known as an affine transformation. As previously stated, the input frame's fabric may experience shearing or translation even if the capturing camera and input frame are maintained in the ideal location. Consequently, affine transformation is performed on the input image frame [17]. The produced transformed image will be utilized in the subsequent steps.

Guided Filter

The border pixels need to be improved in order to improve the edge detection process. This enhancement is perfectly made possible by the linear translation-variant guided filtering procedure [18]. The parameters of the filtering procedure are the guidance image and the filtering input image. Based on the function that was mentioned earlier in the reference, both and are identical in our work. A weighted average is the way the filtering results at a pixel are expressed:

$$M_i = \sum_j W_{ij}(I) K_j \qquad (1)$$

where i and j are represents the pixel indices. M is the filtered image filtered with the filtering kernel W_{ij}, which is linear with respect to K.

II. BERKELEY EDGE DETECTOR

Images of intensity or color can be processed using the Berkeley edge detector [19]. It consolidates variety, splendor and surface prompts to give a probabilistic edge map, where for every pixel in the picture a likelihood of being an edge, or shape is determined. The method looks for local discontinuities at each image pixel across a variety of orientations and scales in several feature channels (such as brightness and texture). Draw a circle with a radius of r at one location in the image and divide it along its diameter at orientation. is the gradient function, which is used to compare the contents of the two disc halves that result. A discontinuity in the image along the diameter of the disc is indicated by a significant difference between the disc halves. Using the X2 difference operator[, the content of the disk halves is represented by binning the selected pixel feature into a histogram, and the disc halves comparison is carried out by comparing the corresponding histograms [20]:

$$x^2(g,h) = 1/2 \sum {(g_i - h_i)^2} \Big/ {g_i + h_i} \qquad (2)$$

The three features chosen are brightness, texture, and, as previously stated. The detector makes use of the CIE L*a*b* feature space. Consequently, brightness is represented by the luminance component L*, and colors are represented by the chrominance components a* and b*. For improved accuracy at a low computational cost, the color gradient is calculated as the sum of the gradients in the a* and b* axes instead of the joint histogram. For the texture gradient, histograms of vector quantized filter outputs are calculated and compared. A logistic regression model that learns multiple oriented and scaled features is used to calculate the final edge probability for each pixel. The edge pixels are kept for later feature extraction when a threshold is activated.

III. CONTOUR BASED FEATURE EXTRACTION

To get familiar with the primary properties of a texture outline, the shape based highlights are mean a lot to remove. Many contour-based features have impressed us. where only a few notable descriptors are taken into consideration. We've looked at twelve different types of descriptors in total, including, but not limited to, the Minimum Bounding Rectangle, the Circle Variance, the Circularity Ratio, the Convexity, the Rectangularity, the Cumulative Angular Deviant, the Contour Curvature, the Ellipse Variance, the Average Bending Energy, the Boundary Moments, the Beam Angle Statistics, and the Chord Distribution [21]. These feature vectors are utilized during the defect detection procedure.

Minimum bounding rectangle

The minimum bounding rectangle is also called minimum bounding box. It is the smallest rectangle that contains every point in the extracted fabric frame. For an arbitrary shape, eccentricity is the ratio of the length L and width W of the minimal bounding rectangle of the shape at some set of orientations. Elongation, Elo, is another concept based on eccentricity. Elongation is a measure that takes values in the range [0; 1]. Asymmetrical shape in all axes such as a circle or square will have an elongation value of 0 whereas shapes with large aspect ratios will have an elongation closer to 1.

$$Elo = 1 - W / L \tag{3}$$

Circularity ratio

Circularity ratio represents how a fabric shape is similar to a circle. There are two definitions: Circularity ratio is the ratio of the area of the fabric frame to the area of a circle having the same perimeter:

$$C_1 = \frac{A_s}{A_c} \tag{4}$$

Where A_s is the area of the extracted frame and A_c is the area of the circle having the same perimeter as the frame. Assume the perimeter is O, so $A_c = O^2/4\pi$. Then $C_1 = 4\pi . A_s / O^2$. As 4π is a constant, so we have the second circularity ratio definition.Circularity ratio is the ratio of the area of a shape to the shape's perimeter square:

$$C_2 = \frac{A_s}{O^2} \qquad (5)$$

Circle variance

The circle variance of the fabric frame is defined as:

$$C_{va} = \frac{\sigma_R}{\mu_R} \qquad (6)$$

where are the mean and standard deviation of the radial distance between the frame's centroid and the boundary points, respectively; $(x_i, y_i); i \in [0, N-1]$.They are the following formulae respectively:

$$\mu_R = \frac{1}{N}\sum_{i=1}^{N-1} d_i \qquad (7)$$

$$\sigma_R = \sqrt{\frac{1}{N}\sum_{i=1}^{N-1}(d_i - \mu_R)^2} \qquad (8)$$

where $d_i = \sqrt{(x_i - g_x)^2 + (y_i - g_y)^2}$ So the most compact shape is a circle.

Convexity

Convexity is defined as the ratio of perimeters of the convex hull $O_{convexhull}$ over that of the original fabric frame contour O

$$convexity = \frac{O_{convexhull}}{O} \qquad (9)$$

The region R^2 is convex if and only if for any two points $P_1 P_2 \in R^2$ the whole line segment $P_1 P_2$ is inside the region. The convex hull of a region is the smallest convex region including it.

Rectangularity

The degree to which the fabric frame fills its minimum bounding rectangle is referred to as its rectangularity: $Rectangularity = \frac{A_s}{A_R}$ (10)

where A_s is the area of a fabric frame; A_R is the area of the minimum bounding rectangle of fabric frame A_s.

The cumulative angular deviant function is a periodic function that is defined as (11) where N is the total number of contour points.

$$\psi(t) = \varphi(\frac{N}{2\pi}t) - t \quad t \in [0,2\pi] \tag{11}$$

where N is the total number of contour points.

Shape curve

The curve is a vital limit highlight for anybody to pass judgment on closeness between shapes. Additionally, it has proven to be extremely helpful for shape recognition and possesses prominent perceptual characteristics. We quote the function of curvature, K(n), from [22 & 23] as follows for the purpose of utilizing K(n) for shape representation:

$$K(n) = \frac{\dot{x}(n)\ddot{y}(n) - \dot{y}(n)\ddot{x}(n)}{\left(\dot{x}(n)^2 + \dot{y}(n)^2\right)^{3/2}} \tag{12}$$

As a result, the parametric representation of a planar curve can be used to calculate the curve's curvature. The previous equation can be written as follows if is the normalized arc-length parameter s:

$$K(s) = \dot{x}(s)\ddot{y}(s) - \dot{y}(s)\ddot{x}(s) \tag{13}$$

The curvature function is invariant under rotations and translations because it is only calculated from parametric derivatives, as shown in the equation above. The curvature measure, on the other hand, is scale dependent—that is, it is inversely proportional to the scale. We can preserve scale independence, i.e., by normalizing this measure by the mean absolute curvature. By normalizing this measure by the mean absolute curvature we can archive scale independence, i.e.,

$$K'(s) = \frac{K(s)}{\frac{1}{N} \quad \sum_{s=1}^{N} |K(s)|} \tag{14}$$

where N is the number of points on the normalized contour.When the size of the curve is an important discriminative feature, the curvature should be used without the normalization; otherwise, for the purpose of scale-invariant shape analysis, the normalization should be performed. An approximate arc-length parameterization based on the centripetal method is given by the following [23]:

Let $P=\sum_{n=1}^{N} d_n$ be the perimeter of the curve and $L=\sum_{n=1}^{N}\sqrt{d_n}$, where d_n is the length of the chord between points p_n and $p_{n+1}, n=1,2....,N-1$. The approximate arc-length parameterization relations: $s_1=0$

$s_k=s_{k-1}+\frac{P\sqrt{d_k-1}}{L}, k=2,3,...N$ (15)Starting from an arbitrary point and following the contour clockwise, we compute the curvature at each interpolated point using Eq. 15. Evidently, as a descriptor, the curvature function can distinguish different shapes.

Ellipse variance

Ellipse variance Eva is a mapping error of a shape to fit an ellipse that has an equal covariance matrix as the shape[21]:

$$C=\frac{1}{N}\sum_{i=0}^{N-1}\begin{pmatrix} x_i-g_x \\ y_i-g_y \end{pmatrix}\begin{pmatrix} x_i-g_x \\ y_i-g_y \end{pmatrix}^T=\begin{pmatrix} c_{xx} & c_{xy} \\ c_{yx} & c_{yy} \end{pmatrix} \quad (16)$$

Where

$c_{xy}=\frac{1}{N}\sum_{i=0}^{N-1}(x_i-g_x)(y_i-g_y)$ $c_{xx}=\frac{1}{N}\sum_{i=0}^{N-1}(x_i-g_x)^2$, $c_{yx}=\frac{1}{N}\sum_{i=0}^{N-1}(y_i-g_y)(x_i-g_x)$

$c_{yy}=\frac{1}{N}\sum_{i=0}^{N-1}(y_i-g_y)^2$ and $C_{ellipse}=C$, It is practically effective to apply the inverse approach yielding. We assume $V_i=\begin{pmatrix} x_i-g_x \\ y_i-g_y \end{pmatrix}$, $d'_i=\sqrt{V_i^T\cdot C_{ellipse}^{-1}\cdot V_i}$, $\mu'_R=\frac{1}{N}\sum_{i=1}^{N-1}d'_i$

and $\sigma'_R=\sqrt{\frac{1}{N}\sum_{i=1}^{N-1}(d'_i-\mu'_R)^2}$ Then

$$E_{va}=\frac{\sigma'_R}{\mu'_R} \quad (17)$$

Comparing with circularity ratio, Ellipse variance E_{va} represents a fabric frame more accurately than circularity ratio.

Average bending energy

Assuming that K(s) is the arc length parameter, the number of points on a contour, and the curvature function [24], the average bending energy is defined as

$$BE = \frac{1}{N}\sum_{s=0}^{N-1} K(s)^2 \quad (18)$$

Young et al. were able to more accurately calculate the average bending energy by using al. [25] used Parseval's relation and Fourier coefficients to perform the boundary's Fourier transformation.

Boundary moments

The advantage of boundary moment descriptors is that it is easy to implement. However, it is difficult to associate higher order moments with the physical interpretation of the fabric frame. The Boundary moments, analysis of a contour, can be used to reduce the dimension of boundary representation [24]. Assume shape boundary has been represented as a 1-D shape representation $z(i)$ as introduced, the r^{th} moment m_r and central moment μ_r can be estimated as

$$m_r = \frac{1}{N}\sum_{i=1}^{N}[z(i)]^r \quad (19)$$

$$\mu_r = \frac{1}{N}\sum_{i=1}^{N}[z(i)-m_1]^r \quad (20)$$

where N is the number of boundary points. The normalized moments $\overline{m}_r = m_r/(\mu_2)^{r/2}$ and $\overline{\mu}_r = \mu_r/(\mu_2)^{r/2}$ are invariant to shape translation, rotation and scaling. Less noise-sensitive shape descriptors of the fabric frame can be obtained from

$$F_1 = \frac{(\mu_2)^{r/2}}{m_1}, F_2 = \frac{\mu_3}{(\mu_2)^{3/2}}, F_3 = \frac{\mu_4}{(\mu_2)^2} \quad (21)$$

Beam angle statistics

A fabric boundary point serves as the basis for the beam angle statistics (BAS) shape descriptor [27]. Using statistical data derived from the beams of individual points, the beam angle statistics shape descriptor captures perceptual data. By utilizing all other boundary points, it provides each boundary point with globally discriminative features. The BAS descriptor is also invariant to translation, rotation, and scaling and very stable under distortions. Let B be the fabric boundary. $B = \{P_1, P_2, \ldots P_N,\}$ is represented by a connected sequence of points, $P_1 = (x_i, y_i)$, $i = 1,2,\ldots N,$ where N is the number of boundary points. For each point P_i , the beam angle between the forward beam vector $v_{i+k} = \overrightarrow{p_i p_{i+k}}$ and backward beam vector $v_{i-k} = \overrightarrow{p_i p_{i-k}}$ in the k^{th} order neighbor-hood system is then computed as

$$C_k(i) = \left(\theta v_{i+k} - \theta v_{i-k}\right) \quad (22)$$

where $\theta v_{i+k} = \arctan \dfrac{y_{i+k} - y_i}{x_{i+k} - x_i}$ and $\theta v_{i-k} = \arctan \dfrac{y_{i-k} - y_i}{x_{i-k} - x_i}$ For each boundary point p_i of the contour, the beam angle $C_k(i)$ can be taken as a random variable with the probability density function $p(C_k(i))$. Therefore, the fabric frame compact representation can be provided by beam angle statistics (BAS).

Chord distribution

By calculating the lengths of all chords in the shape—that is, all pair-wise distances between boundary points—the chord distribution is created as a "lengths" histogram that scales linearly with the object's size and is invariant to rotation [25]. The highest 10 bin values are the features descriptors that more precisely distinguish the fabric frame.

IV. DEFECT DETECTION PROCESS

After the feature vector is extracted from the fabric frame, these features are used by the defect detection process framework. For this purpose, the KNN classification algorithm is utilized. KNN is an instance-based learning classifier that classifies data by using the closest data point in feature space. Consider the X: training data, Y: class names of X, x: obscure illustrations The littlest k distance test's names are processed as set S, so S is the subset of Y. The greater part mark y is recognized as the class, where D is the distance vector among X and x.

The fitted KNN classifier in our framework is taken care of the extricated elements to find the texture imperfection. We have implemented and compared a few more supervised classifiers, including SVM, RBM, and ELM [26].

4. Experimental Results

The experimental setup, as well as the outcomes and analysis of the proposed method for the classification problem of fabric defect detection, are discussed in this section. The natively collected fabric image data set served as the basis for the experiments. The contour frame harmonizing techniques were used to examine the images. The performance of the KNN classifier has been evaluated through training and testing with contour-based features. MATLAB is used to implement the proposed system. The Windows 8.1 computer used for the training and testing has an Intel Core I3 CPU running at 2.3 GHz, 2 GB of RAM, and 250 GB of storage.

We have concentrated on the distinction between normal and defected fabric defects in this work. Based on the extracted feature descriptors, the training process consistently uses the dataset's standard parts of fabric types. The abandoned underlying properties of the texture parts are likewise educated by the classifier utilizing the deserted examples. In order to train the system, 64 different kinds of fabric parts were used, including 320 standards with no defects and 320 images with defects. The test set consists of 420 images, 190 of which are Defected and 230 of Normal. The random sampling method is used to evolve the test sets. The classification results using the KNN classifier are presented in this section. For the classification of training and test data, the confusion matrices are provided.

The confusion matrices gathered during the testing phase are presented in Table I. It is evident from the confusion matrices that the proposed method produces favorable test set outcomes. The test set's classification results are precise. The matrices also make it abundantly clear that, despite the fact that the proposed method improves classification accuracy for fabric defects, Due to the presence of additional curvatures in the fabric frame, the observation leads to the misclassification of non-defective fabric frames as defective. A similar situation is likewise seen in the bogus positive cases.

Statistical performance metrics like sensitivity, specificity, F-score, precision, and accuracy are used to evaluate the proposed architecture (Figure 1). We created the comparison between our proposed architecture and SVM, RBM, and ELM, three other approaches. Table 2 contains a rundown of all the presentation pointers. Together with the other analyzed classifiers, the grouping implementation of our proposed strategy was depicted in Figure 2. In these evaluations, the various analyses employ the same feature descriptors. The proposed approach was able to achieve 96.09 percent sensitivity, 94.74 percent specificity, 95.67 percent precision, 95.48 percent accuracy, and a F score of 95.88 percent throughout the course of the experiment.

Table 1: Confusion matrices obtained to evaluate the system while testing.

		Classified Type	
		Normal	**Defected**
Test Set	**Normal**	221	9
	Defected	10	180

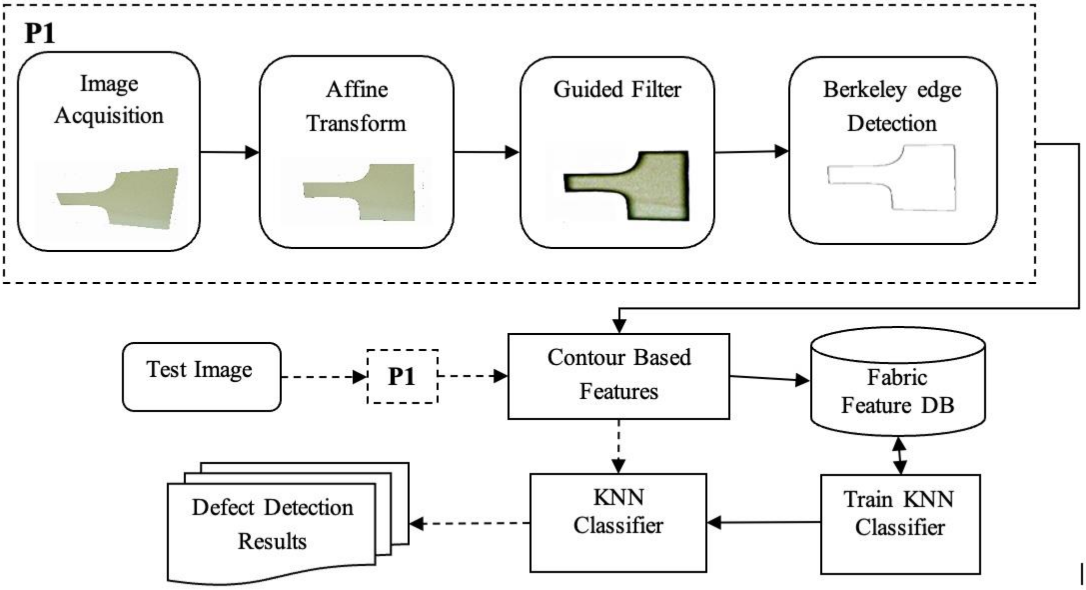

Figure 1: System Architecture.

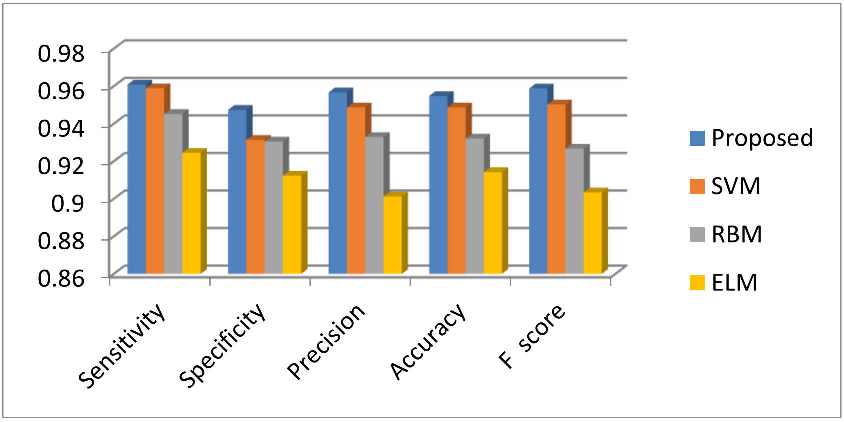

Figure 2: compared and illustrated the effectiveness of our proposed method in classification with that of other classifiers.

Table 2: Test set performance metrics for the proposed work and other classifiers.

Classifier	Sensitivity	Specificity	Precision	Accuracy	F score
Proposed	0.9609	0.9474	0.9567	0.9548	0.9588
SVM	0.9589	0.9314	0.9487	0.9487	0.9503
RBM	0.9452	0.9305	0.9329	0.9321	0.9267
ELM	0.9245	0.9123	0.9012	0.9142	0.9034

5. Conclusion

Computer-aided image analysis for the classification of fabric defects is proposed in this work. Computational methods that make use of a variety of image processing techniques are used in this analysis. Transformation and filtering techniques are used to pre-process the fabric image frame that is input. The edge map is extracted using the standard outline extraction technique with the Berkeley edge detector. The KNN classifier extracts and categorizes contour-based features. The trial and error with local informational index created the extraordinary execution results when contrasted and different classifiers. Our subsequent work centered on frame-matching methods for locating the fabric frame flaw.

References

[1] Damage Detection in Composite Materials Using Lamb Wave Methods ,Seth S. Kessler and S. Mark Spearing Department of Aeronautics and Astronautics, Massachusetts Institute of Technology, Cambridge, MA 02139, USA

[2] Bodnarova, A., M. Bennamoun, and K. K. Kubik, Defect detection in textile materials based on aspects of the HVS, In *Systems, Man, and Cybernetics, 1998. 1998 IEEE International Conference on,* 5 (1998) 4423-4428. https://doi.org/10.1109/ICSMC.1998.727546

[3] Automatic Structure Analysis and Objective Evaluation of Woven Fabric Using Image Analysis TAE JIN KANG, So0 HYUN CHOI, AND SUNG MIN KIM Department of Fiber arid Polytner Science, Seoiil National University, Seoril, Soiith Korea KYUNG WHA OH Department of Honte Economics Education, Cliung-Ang University, Seoiil, Soiith Korea

[4] M. Shi, R. Fu, Y. Guo, S. Bai, & B. Xu, Fabric defect detection using local contrast deviations. *Multimedia Tools and Applications, 52*(1) (2011) 147

[5] Mak, Kai-Ling, P. Peng, and K. F. C. Yiu, Fabric defect detection using morphological filters, *Image and Vision Computing* 27(10) (2009) 1585-1592. https://doi.org/10.1016/j.imavis.2009.03.007

[6] Cawley, Peter, and R. D. Adams, The location of defects in structures from measurements of natural frequencies, *The Journal of Strain Analysis for Engineering Design* 14(2) (1979) 49-57. https://doi.org/10.1243/03093247V142049

[7] N. Tandon, and A. Choudhury, A review of vibration and acoustic measurement methods for the detection of defects in rolling element bearings, *Tribology international* 32(8) (1999) 469-480. https://doi.org/10.1016/S0301-679X(99)00077-8

[8] P. M. Mahajan, S. R. Kolhe, and P. M. Patil, A review of automatic fabric defect detection techniques, *Advances in Computational Research* 1(2) (2009) 18-29.

[9] Kumar, Ajay, and Grantham KH Pang, Defect detection in textured materials using Gabor filters, *IEEE Transactions on Industry Applications* 38(2) (2002) 425-440. https://doi.org/10.1109/28.993164

[10] Chan, Chi-ho, and Grantham Pang, Fabric defect detection by Fourier analysis." In *Industry Applications Conference, 1999. Thirty-Fourth IAS Annual Meeting. Conference Record of the 1999 IEEE,* 3 (1999) 1743-1750. http://dx.doi.org/10.1109/IAS.1999.805975

[11] Tsai, Du-Ming, and Tse-Yun Huang, Automated surface inspection for statistical textures, *Image and Vision Computing* 21(4) (2003) 307-323. https://doi.org/10.1016/S0262-8856(03)00007-6

[12] Tsai, Du-Ming, and Cheng-Huei Chiang, Automatic band selection for wavelet reconstruction in the application of defect detection, *Image and Vision Computing* 21(5) (2003) 413-431. https://doi.org/10.1016/S0262-8856(03)00003-9

[13] K.L. Mak, and P. Peng, An automated inspection system for textile fabrics based on Gabor filters, *Robotics and Computer-Integrated Manufacturing* 24(3) (2008) 359-369. https://doi.org/10.1016/j.rcim.2007.02.019

[14] Cho, Che-Seung, Byeong-Mook Chung, and Moo-Jin Park, Development of real-time vision-based fabric inspection system, *IEEE Transactions on Industrial Electronics* 52(4) (2005) 1073-1079. https://doi.org/10.1109/TIE.2005.851648

[15] Seth S Kessler, S Mark Spearing and Constantinos Soutis. Damage detection in composite materials using Lamb wave methods, *Smart Materials and Structures,* 11(2) (2002) 269. https://doi.org/10.1088/0964-1726/11/2/310

[16] Abouelela, Ahmed, Hazem M. Abbas, HeshamEldeeb, Abdelmonem A. Wahdan, and Salwa M. Nassar, Automated vision system for localizing structural defects in textile fabrics, *Pattern Recognition Letters* 26(10) (2005) 1435-1443. https://doi.org/10.1016/j.patrec.2004.11.016

[17] Zhang, GuiMei, JiYuan Xu, and Jian Xin Liu, A new method for recognition partially occluded curved objects under affine transformation, In *Intelligent Systems and Knowledge Engineering (ISKE), 2015 10th International Conference on*, pp. 456-461. IEEE, 2015. https://doi.org/10.1109/ISKE.2015.52

[18] He, Kaiming, Jian Sun, and Xiaoou Tang, Guided image filtering, *IEEE Transactions on Pattern Analysis and Machine Intelligence,* 35(6) (2013) 1397-1409. https://doi.org/10.1109/TPAMI.2012.213

[19] D. R. Martin, C. C. Fowlkes, and J. Malik, Learning to detect natural image boundaries using local brightness, color, and texture cues, *IEEE Transactions on Pattern Analysis and Machine Intelligence*, 26(5), (2004) 530–549. https://doi.org/10.1109/TPAMI.2004.1273918

[20] J. Puzicha, Y. Rubner, C. Tomasi, and J. Buhmann, Empirical Evaluation of Dissimilarity Measures for Color and Texture, Proceedings of the Seventh IEEE International Conference on Computer Vision, 2 (1999) 1165-1172. https://doi.org/10.1109/ICCV.1999.790412

[21] Mingqiang Yang, KidiyoKpalma, Joseph Ronsin, A Survey of Shape Feature Extraction Techniques, Peng-Yeng Yin. Pattern Recognition, IN-TECH, pp.43-90, 2008.

[22] F. Mokhtarian and A. K. Mackworth, A theory of multiscale, curvature-based shape representation for planar curves, IEEE Transactions on Pattern Analysis and Machine Intelligence, 14(8) (1992) 789-805. https://doi.org/10.1109/34.149591

[23] A. C. Jalba, M. H. F. Wilkinson, and J. B. T. M. Roerdink, Shape representation and recognition through morphological curvature scale spaces, IEEE Transactions on Image Processing, 15(2)(2006) 331-341. https://doi.org/10.1109/TIP.2005.860606

[24] S. Loncaric, A survey of shape analysis techniques, Pattern Recognition, 31(8) (1998) 983 -1001. https://doi.org/10.1016/S0031-2023(97)00122-2

[25] O. Koller, N.C. Camgoz, H. Ney, & R., Bowden, Weakly supervised learning with multi-stream CNN-LSTM-HMMs to discover sequential parallelism in sign language videos, IEEE transactions on pattern analysis and machine intelligence, 42(9) (2019) 2306-2320. https://doi.org/10.1109/TPAMI.2019.2911077

[26] S.Y. Kim, H.G. Han, J.W. Kim, S. Lee & T.W. Kim, A hand gesture recognition sensor using reflected impulses, IEEE Sensors Journal, 17(10) (2017) 2975-2976. https://doi.org/10.1109/JSEN.2017.2679220

Funding

No funding was received for conducting this study.

Conflict of interest

The Authors have no conflicts of interest to declare that they are relevant to the content of this article.

About The License